ACS OMEGA

http://pubs.acs.org/journal/acsodf

Article

Identification of the Neoaspergillic Acid Biosynthesis Gene Cluster by Establishing an *In Vitro* CRISPR-Ribonucleoprotein Genetic System in *Aspergillus melleus*

Bo Yuan, Michelle F. Grau, Ramiro Mendonça Murata, Tamas Torok, Kasthuri Venkateswaran, Jason E. Stajich, and Clay C. C. Wang*

Cite This: *ACS Omega* 2023, 8, 16713−16721

Read Online

ACCESS | Metrics & More | Article Recommendations | Supporting Information

ABSTRACT: Filamentous fungi are an essential source of bioactive mycotoxins. Recent efforts have focused on developing antifungal agents that are effective against invasive yeasts, such as *Candida* spp. By screening fungal strains isolated from regions surrounding the Chernobyl nuclear power plant disaster for antifungal activity against *Candida albicans*, we found that *Aspergillus melleus* IMV 01140 produced compounds that inhibited the growth of the yeast. The active compound produced by *A. melleus* was isolated and found to be neoaspergillic acid, a compound that is closely related to aspergillic acid. While aspergillic acid and its derivatives have been characterized and were found to have antibacterial and antifungal properties, neoaspergillic acid has been much less studied. Even though neoaspergillic acid and related compounds were found to have antibacterial and antitumoral effects, further investigation into this group of compounds is limited by challenges associated with large-scale production, isolation, and purification. The production of neoaspergillic acid has been shown to require co-cultivation methods or special growth conditions. In this work, neoaspergillic acid and related compounds were found to be produced by *A. melleus* under laboratory growth conditions. The biosynthetic gene cluster of neoaspergillic acid was predicted using the aspergillic acid gene cluster as a model. The biosynthetic pathway for neoaspergillic acid was then confirmed by establishing an *in vitro* CRISPR-ribonucleoprotein system to individually delete genes within the cluster. A negative transcriptional factor, *mcrA*, was also eliminated to further improve the production of neoaspergillic acid and the related compounds for future studies.

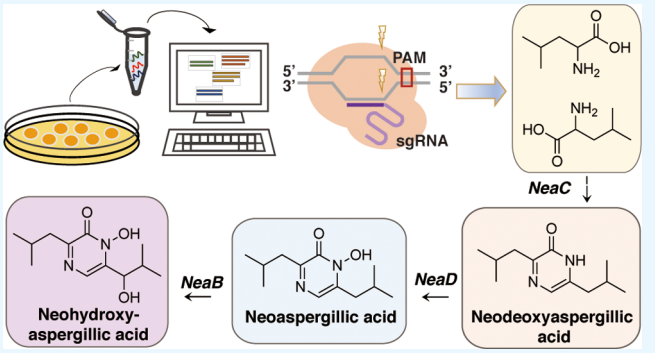

INTRODUCTION

Candida yeasts, such as *Candida albicans*, are invasive species that can be deadly in immunocompromised patients.[1] With the limited number and activities of antifungal therapies, it is crucial to discover more antifungal drugs that can successfully treat Candida infections.[2,3] The investigation of fungal secondary metabolites (SMs) has progressed rapidly with the recent development of molecular genetic tools. SMs have been used extensively in the agricultural, food, cosmetic, and pharmaceutical industries.[4−6] As the number of sequenced fungal genomes has rapidly increased, efficient techniques have been developed that make fungal strains genetically more accessible.[7,8] Among various gene manipulation methods, CRISPR (clustered regularly interspaced short palindromic repeat)-Cas9 has been shown to achieve extremely accurate and efficient edits. Adaptation of the CRISPR gene editing technology has revealed unknown SM biosynthetic pathways in several filamentous fungi.[9−12]

In our screen of over 150 fungal strains for the production of compounds with anti-*Candida* activity, *Aspergillus melleus* was found to produce a compound that exhibits growth inhibition of *C. albicans*. Compound isolation, followed by NMR structural determination, identified the antifungal activities as neoaspergillic acid. Aspergillic acid and related compounds have been widely studied as mycotoxins, with many of them displaying antibacterial and antifungal activities.[13,14] While the gene cluster and biosynthetic pathway of aspergillic acid have been reported, there are limited studies about a closely related compound, neoaspergillic acid.[13] Previous investigations have shown that neoaspergillic acid possesses antibacterial, antifungal, and antitumoral effects.[15,16] With relatively strong toxicity, the lethal dose (LD50) of neoaspergillic acid in mice

Received: December 20, 2022
Accepted: March 9, 2023
Published: May 1, 2023

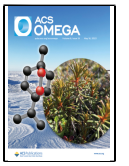

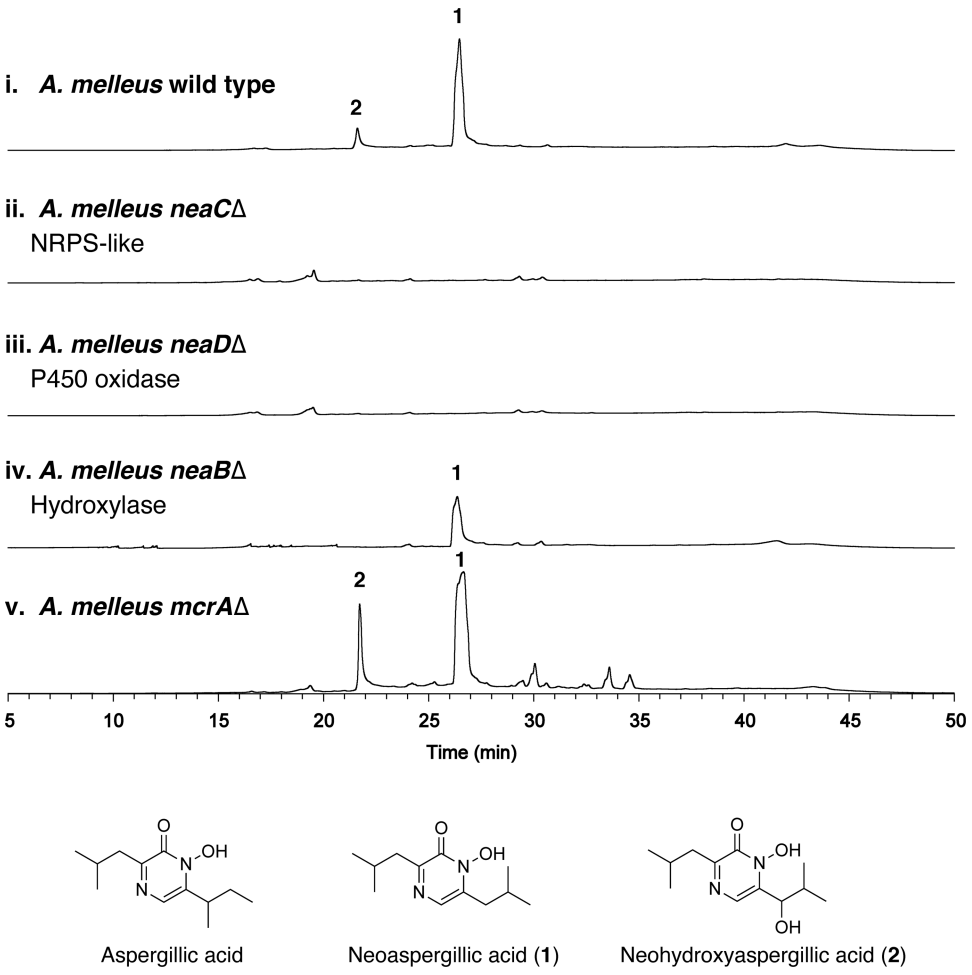

Figure 1. Paired HPLC profiles of *A. melleus* (wild type, *neaC*Δ, *neaD*Δ, *neaB*Δ, *mcrA*Δ strains) extracts when grown on a solid YEPD medium: (i) wild type, (ii) *neaC*Δ, (iii) *neaD*Δ, (iv) *neaB*Δ, and (v) *mcrA*Δ strains.

was reported to be 125 mg/kg.[17] The complex derivatives of this compound, such as ferrineoaspergillin, aluminiumneoaspergillin, and zirconiumneoaspergillin, also acquire different levels of toxic activities.[14,18,19] A dimeric zinc complex, dizinchydroxyneoaspergillin was also found to have significant bactericidal effects on methicillin-resistant bacteria strains.[20] In our optimized laboratory conditions, the highest titer we could obtain is 4 mg/L neoaspergillic acid from liquid culture. To enable the production of sufficient quantities of this antifungal compound for derivatization and further development as an anti-*Candida* agent, we set out to identify the genes involved in the biosynthesis of neoaspergillic acid. We confirmed the gene cluster that is responsible for producing neoaspergillic acid by establishing an *in vitro* CRISPR-Cas9 system in *A. melleus* with assembled ribonucleoprotein (RNP). The nonribosomal peptide synthetase (NRPS)-like core gene and tailoring enzymes such as the P450 oxidase and hydrolase have been deleted individually to validate the biosynthetic pathway of this compound. In our initial attempt to increase the titer of neoaspergillic acid, we deleted a negative transcriptional factor, *mcrA*, in *A. melleus* using the same *in vitro* CRISPR-Cas9 system. Upregulation of both neoaspergillic acid (**1**) and neohydroxyaspergillic acid (**2**) in the *mcrA*Δ strain was observed, indicating that this gene cluster was negatively regulated by *mcrA* in *A. melleus*.

RESULTS

***A. melleus* Produces Neoaspergillic Acid on a Solid YEPD Medium. The Gene Cluster Was Located through Sequence Analysis of the Genome and Gene Annotation.** Over 150 fungal strains collected from the Chernobyl nuclear power plant and surrounding areas were screened for antifungal activity against *C. albicans* ATCC 90028 and fluconazole-resistant *C. albicans* ATCC 321182. The selected strains were designated by IMV (Institute of Microbiology and Virology, Kiyv, Ukraine) strain numbers. Among the fungal species with antifungal activity against *C. albicans*, *A. melleus* IMV 01140 was found to produce two compounds on solid Yeast Extract Peptone Dextrose (YEPD) medium as analyzed by liquid chromatography−mass spectrometry (LC-MS) (Figure S1). To identify the compounds, *A. melleus* was cultivated on 15 cm diameter Petri dishes in multiple replicates (n = 40) of YEPD medium, and the compounds were purified by a solid−liquid extraction, column chromatography, and high-performance liquid chromatography (HPLC). The two major compounds produced were confirmed to be neoaspergillic acid (**1**) and neohydroxyaspergillic acid (**2**) by nuclear magnetic resonance (NMR) analysis (Figures 1 and S2−S4). Compound **3**, a substance related to neoaspergillic acid, was also detected in lower amounts and was predicted to be neodehydroxyaspergillic acid as it shares the same mass with deoxyaspergillic acid in the aspergillic acid pathway.

https://doi.org/10.1021/acsomega.2c08104
ACS Omega 2023, 8, 16713−16721

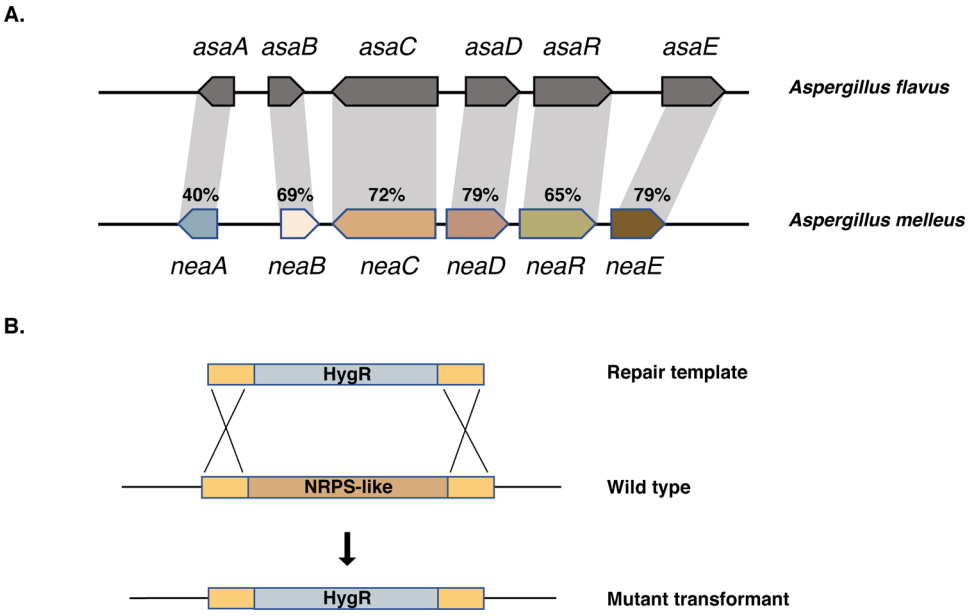

Figure 2. Replacement of the native NRPS-like gene (*neaC*) with a hygromycin resistance (HygR) marker. (A) Predicted neoaspergillic acid gene cluster in *A. melleus* compared with aspergillic acid gene cluster in *A. flavus*. (B) Repair template, consisting of a hygromycin resistance gene (1375 bp), was amplified from plasmid pFC332 with 50 bp flanking regions at both ends. The replacement of the NRPS-like gene (*neaC*) by the HygR marker was induced by DNA cleavages during transformation.

After confirming that neoaspergillic acid was the major compound produced by *A. melleus* on YEPD, we wanted to locate the neoaspergillic acid gene cluster to reveal the biosynthetic pathway. The genome of *A. melleus* IMV 01140 was sequenced and annotated (Figure S5, Tables S1 and S2). Due to the similarity between neoaspergillic and aspergillic acid, we used *asaC*, a nonribosomal peptide synthetase-like (NRPS-like) core gene in the aspergillic acid gene cluster (*Aspergillus flavus* NRRL3357) as a probe to search for the gene cluster of neoaspergillic acid in *A. melleus* (Figures 1 and 2). The homologue of *asaC* protein was identified in the *A. melleus* IMV 01140-predicted proteome using BLASTp (RRID: SCR_001010). The gene cluster of neoaspergillic acid in *A. melleus* had a strong similarity to the gene cluster of aspergillic acid in *A. flavus*, except for the homologues of *asaD* and *asaR*, which were initially predicted together in *A. melleus* (Figure 2A, and Table S3). We designated the homologue of *asaC* in *A. melleus* to be *neaC* and used this name in the following work.

Deletion of *neaC* Using *In Vitro* CRISPR-Cas9 Confirms the Gene Cluster of Neoaspergillic Acid in *A. melleus*. We established an *in vitro* CRISPR-Cas9 system in *A. melleus* to verify that the gene cluster identified by bioinformatics was responsible for producing neoaspergillic acid. DNA repair normally occurs through nonhomologous end joining (NHEJ) when Cas9 introduces a double-strand break in DNA. As NHEJ requires a dimeric protein complex, Ku, to facilitate the repair, genetic manipulations involving entire gene deletions are typically performed in fungal strains with a *Ku-* background. However, by targeting both ends of a gene simultaneously with a microhomologous repair template, it increases the efficiency of gene replacement through microhomology-mediated end joining (MMEJ) (Figure 2B). Thus, we can successfully manipulate wild-type fungal genomes using the CRISPR-RNP system that has previously been reported in other *Aspergillus* spp.

We performed an antibiotic resistance test to determine the effective concentration of hygromycin B. 1.0×10^6 wild-type *A. melleus* protoplasts were inoculated into each well with different hygromycin concentrations (0, 0.05, 0.1, 0.2, 0.4, 0.6 mg/mL). The wild-type *A. melleus* was found to be resistant to hygromycin at 0.4 mg/mL (Figure S6). The repair template, amplified from pFC332, contains a hygromycin resistance gene and 50 bp homologous flanking regions at either end. We designed two crRNAs targeting the 5′ untranslated region (UTR) and 3′ UTR of the NRPS-like gene, *neaC*, respectively, to form RNPs by assembling with tracrRNA and Cas9. The targeting regions were followed by PAM (NGG) sequences for efficient Cas9 cleavage. Protospacer sequences were selected by performing a BLASTN (RRID:SCR_001598) search within the *A. melleus* genome to minimize off-target effects.

We delivered assembled RNPs into wild-type *A. melleus* protoplasts along with the repair template during transformation. Transformants appeared on hygromycin-selective plates on day 4 and were restreaked onto nonselective potato dextrose agar (PDA) for conidium harvesting. DNA was extracted from the fungal biomass of each transformant after incubating for 5 days. To confirm the deletions were correct, we designed primers to amplify the *neaC* sequence using both wild-type and transformant DNA. The *neaC* amplicon was approximately 5 kb for the wild-type and 2.7 kb for correct transformants with the gene deleted. The PCR results indicate that *neaC* was successfully deleted in mutant *A. melleus* strains (Figure S7). Wild-type and *neaC*Δ strains were cultivated on YEPD for 6 days, and plates were extracted for metabolomics analysis. As predicted, the production of neoaspergillic acid and related compounds is eliminated in *neaC*Δ strains, confirming that this is the cluster responsible for the production of neoaspergillic acid (Figure 1).

Deletion of Additional Cluster Genes to Reveal the Biosynthetic Pathway of Neoaspergillic Acid. To establish the biosynthetic pathway, we targeted aspergillic

https://doi.org/10.1021/acsomega.2c08104
ACS Omega 2023, 8, 16713−16721

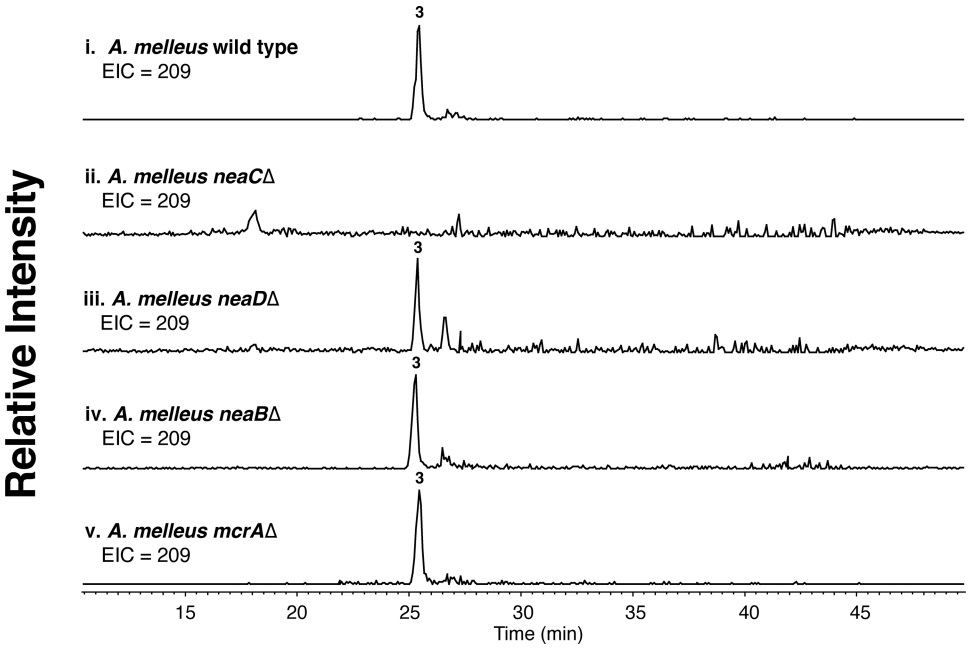

Figure 3. NeaD oxidizes neodeoxyaspergillic acid forming neoaspergillic acid. Extracted ion chromatograms ($[M + H]^+$ = 209) show neodeoxyaspergillic acid (**3**) is present in wild type, *neaD*Δ, *neaB*Δ, and *mcrA*Δ strains extracts when grown on a solid YEPD medium: (i) wild type, (ii) *nea*CΔ, (iii) *neaD*Δ, (iv) *neaB*Δ, and (v) *mcrA*Δ strains.

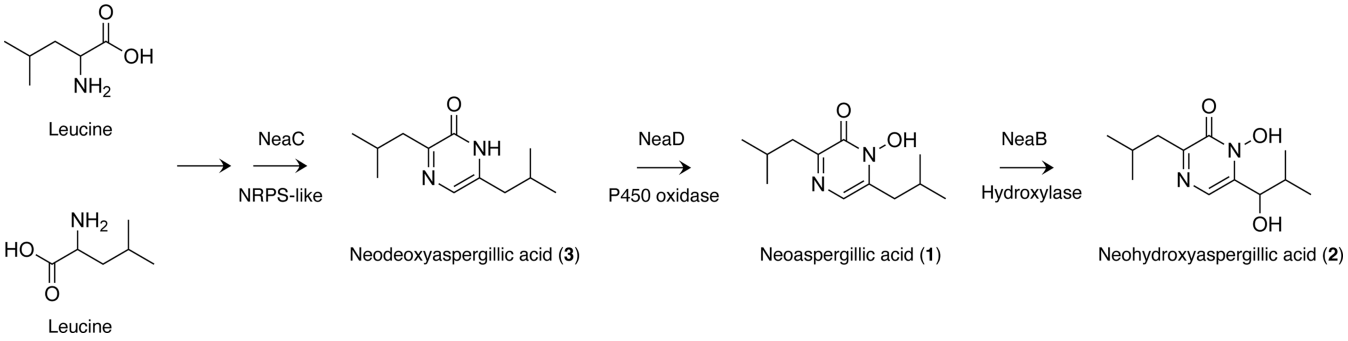

Figure 4. Proposed biosynthesis pathway of neoaspergillic acid in *A. melleus*.

acid homologues of the P450 oxidase (*asaD*) and hydrolase (*asaB*) in the neoaspergillic acid gene cluster. The corresponding genes were located through a BLASTp search and were designated as *neaD* and *neaB*, respectively. Following the same procedure as described above, we designed crRNAs targeting these two genes and assembled them separately with tracrRNA and Cas9. The assembled RNPs were then delivered to wild-type *A. melleus* protoplasts with repair templates during transformation. After 4 days of incubation, transformants were streaked on nonselective PDA plates for conidium collection and DNA extraction. Deletions of *neaD* and *neaB* were confirmed by PCR (Figures S8 and S9).

The *neaD*Δ and *neaB*Δ strains were cultivated on YEPD for 6 days, and plates were extracted for metabolomics analysis. Neoaspergillic acid (**1**) is still produced by *neaB*Δ strains, while neohydroxyaspergillic acid (**2**) is absent, suggesting that *neaB* is responsible for the hydrolysis step following neoaspergillic acid formation (Figure 1iv). Deletion of *neaD* completely abolished the production of both neoaspergillic acid (**1**) and neohydroxyaspergillic acid (**2**) (Figure 1iii). Extracted ion chromatograms (EIC) showed the presence of compound **3** ($[M + H]^+$ = 209 m/z) in wild-type, *neaD*Δ, and *neaB*Δ strains, but not in *neaC*Δ strains. This indicates the formation of compound **3** occurs before the oxidation and hydrolysis steps (Figure 3). An earlier study of the aspergillic acid biosynthetic pathway reports that a compound with the same mass as compound **3** was found by deletion of *asaD* and identified to be deoxyaspergillic acid.[9] Therefore, compound **3** was predicted to be neodeoxyaspergillic acid, and the proposed biosynthetic pathway is illustrated in Figure 4.

Deletion of the Negative Transcriptional Factor, *mcrA*, Upregulates the Production of Neoaspergillic Acid and the Related Compounds. To upregulate neoaspergillic acid production, we decided to target *mcrA*, a negative global regulator of SM production in filamentous fungi. We located the *mcrA* in *A. melleus* using the *A. nidulans mcrA* (AN8694) protein sequence as a probe. The homologue of AN8694 was found in the *A. melleus* genome annotation using BLASTp. We designed crRNAs targeting both ends of the gene and performed RNP assembly and fungal transformation as described before. Transformants were restreaked on PDA plates for conidium harvesting and DNA extraction. Correct transformants were confirmed using PCR that assessed

https://doi.org/10.1021/acsomega.2c08104
ACS Omega 2023, 8, 16713−16721

the presence of the *hygB* marker and the absence of the *mcrA* gene (Figure S10).

Upregulation of both neoaspergillic acid (**1**) and neohydroxyaspergillic acid (**2**) was observed in the HPLC profiles of metabolite extracts from the *mcrA*Δ strain compared to the wild-type strain (Figure 1). We observed a 1.7-fold and 1.6-fold increase in the production of neoaspergillic acid (**1**) and neohydroxyaspergillic acid (**2**), respectively, in *mcrA*Δ strain (Figure 5). Upregulation of neoaspergillic and neohydroxyaspergillic acid in the *mcrA* deletion strains suggests that *mcrA* acts as a negative regulator of the neoaspergillic acid gene cluster. The *mcrA*Δ strain can be utilized to enhance the production of compound **1** for future studies focused on characterizing the biological properties of neoaspergillic acid.

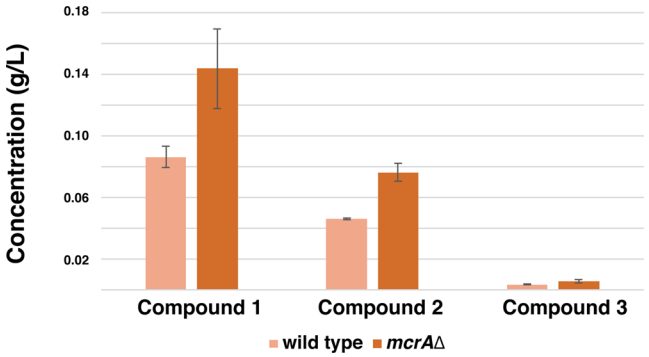

Figure 5. Increased production of compounds **1** and **2** in *mcrA*Δ strain. Neoaspergillic acid (**1**) production increased by 1.7-fold and neohydroxyaspergillic acid (**2**) production increased by 1.6-fold compared to the ones in the wild type (n = 3; data shown are mean ± standard deviation).

CONCLUSIONS AND DISCUSSION

In previous studies,[19−21] the production of neoaspergillic acid has been shown to require co-cultivation of *Aspergillus* species or a monoculture in high salt stress conditions. Cultivation of some other *Aspergillus* species for neoaspergillic acid extraction was as long as 60 days, and purified compounds were mainly isolated through alkali hydrolysis of ferrineoaspergillin, aluminiumneoaspergillin, and zirconiumneoaspergillin.[14,20] The accessibility of neoaspergillic acid limits further studies of its bioactivities and biosynthesis. In this study, neoaspergillic acid and its derivatives were first reported to be produced by *A. melleus* under laboratory growth conditions on day 6 without co-cultivation or the addition of salts. The gene cluster of neoaspergillic acid was predicted using the aspergillic acid cluster core gene, *asaC*, as a probe. We established an *in vitro* CRISPR-Cas9 system in *A. melleus* by deleting the NRPS-like core gene (*neaC*). The function of the predicted P450 oxidase (*neaD*) and hydrolase (*neaB*) within the gene cluster was also confirmed by deleting each gene individually. The fact that a conserved BGC incorporates different amino acids as precursors and generates distinct final compounds makes fungal genetics more interesting, which requires further investigation. The biosynthetic pathway of neoaspergillic acid was first proposed in this study (Figure 4). To optimize the production, we deleted *mcrA*, a negative transcriptional regulator in *A. melleus*, resulting in enhanced production of neoaspergillic acid (**1**) and neohydroxyaspergillic acid (**2**). By establishing the biosynthetic pathway and optimizing the production of neoaspergillic acid, future studies can focus on the biological characteristics of this compound and its chelation with different metals.

METHODS

Genome Assembly and Annotation. Wild-type *A. melleus* IMV 01140 was cultivated on potato dextrose agar (PDA) for 6 days at 26 °C. The PDA plate with *A. melleus* growth was sent to Novogene (Sacramento, CA) for DNA extraction and Illumina library preparation. The library was sequenced on Illumina NovaSeq to produce 4,425,437 paired-end reads (8,850,874 reads total), 1.327 Gb sequence, and ∼37X coverage of the genome.

The Illumina sequencing reads, in FASTQ format, were downloaded from Novogene servers to the High-Performance Computing Center (HPCC) at UC Riverside (https://hpcc.ucr.edu). The genome was assembled through AAFTF v0.2.3, which relies on trimmomatic v0.36 to trim reads and BBMap to filter PhiX and other contamination. Reads were assembled using SPAdes v3.12.0, and vector sequences were removed with vecscreen step relying on BLASTN against a vector sequence database. Bacteria contamination contigs were filtered using sourmash v3.5.0, and the assembly was polished with the short reads using Pilon v1.22.[22−27] Small contigs that were identical to larger ones were removed with 'rmdup' step in AAFTF, which relies on minimap2. The contigs were sorted from largest to smallest and renamed with the 'sort' step in AAFTF. A *de novo* repetitive sequence database was created for the genome using RepeatModeler v1.0.11 and then used to mask the genome with RepeatMasker v4-0-6 and run within the Funannotate pipeline.[28−30] Genes were predicted with Funannotate, which uses inferred gene models from BUSCO v4 to build a training set for *ab initio* predictors SNAP and Augustus.[31−33] In addition, the tool Genemark.HMM+ES self-training was run to generate gene prediction parameters, followed by runs of all three *ab initio* predictors to produce input gene models. Consensus gene models along with additional protein evidence generated by alignment of UniProt/Swiss-Prot database with Diamond.[34,35] Together, these predictions were combined to produce a consensus gene prediction set with EvidenceModeler.[36] The predicted proteins were assigned putative functional annotations from inferred homology based on protein sequence similarity to entries in Pfam, Interpro, CAZyDB, MEROPS, EggNOG, and Uniprot databases.[34,37−42] Predicted Secretion and localization signals were also recorded based on Phobius v1.01 and signalP v4.1 tools. To predict secondary metabolism genes, antiSMASH v4.1.0 was run in Fungi mode.[43] The sequence reads, assembly, and annotation of the strain were deposited at NCBI GenBank under Bioproject PRJNA883727, and the genome is available under accession number JAOPJF000000000. The predicted gene clusters and genome and gene content statistics are summarized in Supporting Tables 1 and 2. All codes used for genomic analysis were deposited in GitHub (https://github.com/stajichlab/AsmAnnot_Aspergillus_melleus_IMV_01140).

Species Assignment for Strain. To confirm and assign the species designation for the IMV 01140 isolate, we used a phylogenetic approach by extracting copies of the BenA/TUB2 (β-tubulin) genes as it has been shown to be a useful marker for *Aspergillus* species identification.[44] The BenA/TUB2 gene was identified in the IMV 1140 genome and searched with BLASTN against the nonredundant (nt) database from NCBI

https://doi.org/10.1021/acsomega.2c08104
ACS Omega 2023, 8, 16713−16721

(2022-09-01) to identify likely candidate species names.[44] The top hits were identified as *Aspergillus melleus*. Additional deposited partial BenA/TUB2 sequences from other *Aspergillus* strains were downloaded from the nt database and aligned together with copies of BenA/TUB2 identified in genomes of related species based on described taxonomy of the genus. The sequences were aligned with MUSCLE v5.1, trimmed with trimal v1.4.1, and a maximum likelihood phylogenetic tree constructed with IQTree v2.2.1 (Figure S5a).[45−47]

To further confirm identity, a phylogenomic analysis using the BUSCO eurotiomycetes_odb10 marker set was performed by running BUSCO v5.4.3, the single-copy genes identified were aligned to get full coding sequence and were aligned with hmmalign v3.2.1, trimmed, and individual gene trees constructed with FastTreeMP v2.1.11 using the PHYling pipeline.[48−51] Individual trees and alignments were scored for evolutionary rates and alignment length using phykit and bioKit to obtain the fastest evolving and longest alignments for input to a partitioned gene analysis with codon models in IQTree v2.2.1.[47,52,53] The top 20 genes were chosen for the partitioned analysis presented although other combinations were examined (Figure S5b).

Molecular Genetic Procedures. Hygromycin B was used as a selectable marker in this work based on the results of the antibiotic resistance test (Figure S6). A 1375-bp HygR microhomology repair template, which spans 320 bp of the *trpC* promoter and 1020 bp of the hygromycin B resistance cassette, was amplified from pFC332 using primers with 50 bp homologous flanking (Table S4). The amplified PCR products were purified by gel extraction, and the final DNA repair templates were eluted with an Elution Buffer (Qiagen, Cat. No. 19086).

The Alt-R-CRISPR-Cas9 components were ordered from Integrated DNA Technologies (IDT). The universal tracrRNA and the crRNA with the designed 20 bp protospacer were prepared as 100 μM stock solutions and stored at −20 °C before use. The Cas9 nuclease was diluted to a final concentration of 1 μg/μL with nuclease-free Cas9 working buffer (20 mM HEPES, 150 mM KCl, pH 7.5) and stored at −20 °C until use. The crRNA and tracrRNA in equal molar concentrations were first assembled to become the guide RNA duplex at a final concentration of 33 μM. The duplex mixture was heated for 5 min at 95 °C and cooled to room temperature before use or stored at −20 °C for long-term use. The Cas9-gRNA ribonucleoprotein complexes were then generated by combining 1.5 μL of each gRNA duplex separately with 11 μL of nuclease-free Cas9 working buffer and 0.75 μL of Cas9. The RNP complexes were formed by incubating the mixtures for 5 min at room temperature. Two RNP complexes targeting both ends of the gene were combined to form a final volume of 26.5 μL before the transformation.

Transformation of *A. melleus*. Fresh conidia of wild-type *A. melleus* were collected from PDA plates after 6 days of incubation at 26 °C. 1×10^8 Conidia of *A. melleus* were inoculated into 50 mL of Potato Dextrose Broth (PDB) in a 250 mL flask and incubated at 30 °C overnight with shaking at 135 rpm. Mycelia were collected by filtration and resuspended in protoplasting buffer, which was prepared by adding 1.2 g of VinoTaste Pro (VTP) in 20 mL of 1.1 M KCl and 0.39 M citric acid monohydrate buffer (pH 5.8, adjusted with 1.1 M KOH). The protoplasting buffer was vortexed for 15 min and centrifuged for 15 min at 1800 × *g*. Together with the filtered mycelia, the supernatant of the protoplasting buffer was filter-sterilized into a 50 mL flask and incubated at 30 °C for 4 h with shaking at 100 rpm. 5 mL of the protoplast suspension was transferred and gently overlaid with 5 mL 0.4 M ST (0.4 M D-sorbitol, 100 mM Tris-HCl, pH 8) into a 15 mL tube. The tube was centrifuged for 15 min at 4 °C and 800 × *g* to separate protoplasts from the mycelial debris. The protoplast layer was collected at the interface and transferred into a new tube. After adding 15 mL of ST (1.0 M D-sorbitol, 50 mM Tris-HCl, pH 8), the suspension was centrifuged at room temperature for 10 min at 800 × *g*. The protoplast pellet was washed with ST and centrifuged at room temperature at 800 × *g* for 10 min. The pellet was then resuspended in STC buffer (1.0 M D-sorbitol, 50 mM $CaCl_2$, 50 mM Tris-HCl, pH 8). 100 μL (approximately 1.0×10^6) of protoplasts were added to the Cas9 RNP mixture (26.5 μL). Approximately 3 μg of the purified repair template and 25 μL of poly(ethylene glycol) (PEG)-$CaCl_2$ buffer (40% [wt/vol] PEG 3350, 50 mM $CaCl_2$, 50 mM Tris-HCl, pH 8) was added immediately after adding protoplasts. The mixture of protoplast, Cas9 RNP, and the repair templates was incubated for 50 min on ice. PEG-$CaCl_2$ (1.25 mL) was added to the protoplast mixture, and the suspension was incubated for 20 min at room temperature. The suspension was brought to 2 mL by adding STC buffer, and 500 μL of suspension was spread on SMM agar plates (GMM supplemented with 1.2 M sorbitol, 1.5% [wt/vol] agar). The SMM plates were incubated at room temperature overnight, and the second layer of top agar (GMM supplemented with 1.2 M sorbitol, 0.7% [wt/vol] agar) with the selected antibiotic was overlaid. The transformed SMM plates were incubated for 4 days at 30 °C for conidium generation.

Culturing and HPLC−DAD-MS Analysis. *A. melleus* strains were incubated at 26 °C on Yeast Extract Peptone Dextrose (YEPD) agar plates. For each strain, 1.0×10^7 conidia were inoculated on a YEPD plate, and 5 plugs (7 mm diameter) were cut out for compound extraction after 6 days of cultivation. The agar plugs were extracted with 5 mL of methanol. After 1 h of sonication, the extract was collected into a clean glass vial, and the agar plugs were extracted again with 5 mL of dichloromethane/methanol (1:1) followed by another 1 h of sonication. The extract was collected into the same glass vial for evaporation through TurboVap LV (Caliper Life-Sciences). The dried residues were dissolved in equal amounts (7 mL) of ethyl acetate (EtOAc) and water. The EtOAc layer was collected into a new glass vial and evaporated with a TurboVap LV. The dried extract was redissolved in 400 μL of dimethyl sulfoxide (DMSO)/methanol (MeOH) (1:4), and 10 μL was injected into LC−DAD-MS for analysis. We used a ThermoFinnigan LCQ Advantage ion trap mass spectrometer with a reversed-phase C_{18} column (Alltech Prevail C_{18}; column, 2.1 by 100 mm; particle size, 3 μm; flow rate 125 μL min^{-1}) to retrieve LC/MS spectra. Solvent A was 5% acetonitrile (MeCN)−H_2O, and solvent B was 95% MeCN−H_2O. Both solvents contained 0.05% formic acid, and the solvent gradient was as follows: 100% solvent A from 0 to 5 min, 0 to 25% solvent B from 5 to 6 min, 25 to 100% solvent B from 6 to 35 min, 100% solvent B from 35 to 40 min, 100 to 0% solvent B from 40 to 45 min, and re-equilibration with 100% solvent A from 45 to 50 min. The MS included a 5.0 kV capillary voltage, 60-arbitrary units flow rate of the sheath gas, 10-arbitrary units of the auxiliary gas, and 350 °C of the ion transfer capillary temperature.

https://doi.org/10.1021/acsomega.2c08104
ACS Omega 2023, 8, 16713−16721

Compound Purification and Characterization. Wild-type *A. melleus* strains were cultivated in 40 of 15 cm diameter Petri dishes with a total volume of 2.5 L of YEPD medium for 5 days at 26 °C. After incubation, the agar was chopped into pieces and extracted with methanol and dichloromethane/methanol (1:1), followed by 1 h of sonication as described above. The liquid residue was evaporated *in vacuo* to lower the total volume and extracted three times with EtOAc. The combined EtOAc layers were evaporated *in vacuo* to generate a crude extract. Silica gel column chromatography was performed using dichloromethane and methanol as eluent, starting with 1% methanol. Neoaspergillic acid (**1**) and neohydroxyaspergillic acid (**3**) were eluted at 3% methanol. Fractions with desired compounds were combined and further separated through preparative HPLC [Phenomenex Luna 5 μm C_{18} (2), 250 × 21.2; flow rate of 5.0 mL min^{-1}; UV detector at 280 nm]. The purified compounds were characterized by nuclear magnetic resonance (NMR) spectral analysis using a Varian Mercury Plus 400 spectrometer.

■ ASSOCIATED CONTENT

Supporting Information

The Supporting Information is available free of charge at https://pubs.acs.org/doi/10.1021/acsomega.2c08104.

NMR spectroscopic data, genome assembly characteristics, and secondary metabolite clusters predicted tables, antibiotic sensitivity tests, and diagnostic PCR amplifications (PDF)

■ AUTHOR INFORMATION

Corresponding Author

Clay C. C. Wang − *Department of Pharmacology and Pharmaceutical Sciences, School of Pharmacy, University of Southern California, Los Angeles, California 90089, United States; Department of Chemistry, University of Southern California, Dornsife College of Letters, Arts, and Sciences, Los Angeles, California 90089, United States;* orcid.org/0000-0003-2955-7569; Email: clayw@usc.edu

Authors

Bo Yuan − *Department of Pharmacology and Pharmaceutical Sciences, School of Pharmacy, University of Southern California, Los Angeles, California 90089, United States;* orcid.org/0000-0003-1462-5688

Michelle F. Grau − *Department of Pharmacology and Pharmaceutical Sciences, School of Pharmacy, University of Southern California, Los Angeles, California 90089, United States;* orcid.org/0000-0001-5930-5552

Ramiro Mendonça Murata − *Department of Foundational Sciences, School of Dental Medicine, East Carolina University, Greenville, North Carolina 27834, United States*

Tamas Torok − *Ecology Department, Lawrence Berkley National Laboratory, Berkeley, California 94720, United States*

Kasthuri Venkateswaran − *Jet Propulsion Laboratory, California Institute of Technology, Pasadena, California 91109, United States*

Jason E. Stajich − *Department of Microbiology and Plant Pathology, University of California Riverside, Riverside, California 92521, United States;* orcid.org/0000-0002-7591-0020

Complete contact information is available at: https://pubs.acs.org/10.1021/acsomega.2c08104

Notes

The authors declare no competing financial interest.

■ ACKNOWLEDGMENTS

This research was supported in part by the Irving S. Johnson fund of the Kansas University Endowment Association, by the H. L. Snyder Medical Foundation, and by the National Institute of Allergy and Infectious Diseases (Grant R21AI127640) to C.C.C.W and R.M. Part of the research described in this manuscript was performed at the Jet Propulsion Laboratory, California Institute of Technology under a contract with NASA and the University of Southern California. 2022 California Institute of Technology Government sponsorship is acknowledged. This research was funded in part by a 2014 Space Biology NNH14ZTT002N award (grant 80NSSC18K0113) to K.V. J.E.S. is a CIFAR Fellow in the program Fungal Kingdom: Threats and Opportunities and partially supported by USDA Agriculture Experimental Station at the University of California, Riverside and NIFA Hatch project CA-R-PPA-5062-H. J.E.S. was partially supported by NIH-NIAID (Grant R01-AI130128 to Robert Cramer, Jr.).

■ REFERENCES

(1) Nathens, A. B.; Rotstein, O. D.; Marshall, J. C. Tertiary peritonitis: clinical features of a complex nosocomial infection. *World J. Surg.* **1998**, *22*, 158−163.

(2) Pianalto, K. M.; Alspaugh, J. A. New Horizons in Antifungal Therapy. *J. Fungi* **2016**, *2*, No. 26.

(3) Roemer, T.; Xu, D.; Singh, S. B.; Parish, C. A.; Harris, G.; Wang, H.; Davies, J. E.; Bills, G. F. Confronting the challenges of natural product-based antifungal discovery. *Chem. Biol.* **2011**, *18*, 148−164.

(4) Keller, N. P. Fungal secondary metabolism: regulation, function and drug discovery. *Nat. Rev. Microbiol.* **2019**, *17*, 167−180.

(5) de Vries, R. P.; Riley, R.; Wiebenga, A.; Aguilar-Osorio, G.; Amillis, S.; Uchima, C. A.; Anderluh, G.; Asadollahi, M.; Askin, M.; Barry, K.; et al. Comparative genomics reveals high biological diversity and specific adaptations in the industrially and medically important fungal genus *Aspergillus*. *Genome Biol.* **2017**, *18*, No. 28.

(6) Chiang, Y.-M.; Wang, C. C. C.; Oakley, B. R. Analyzing Fungal Secondary Metabolite Genes and Gene Clusters. In *Natural Products*; John Wiley & Sons, Ltd, 2014; pp 171−193.

(7) Keller, N. P.; Turner, G.; Bennett, J. W. Fungal secondary metabolism - from biochemistry to genomics. *Nat. Rev. Microbiol.* **2005**, *3*, 937−947.

(8) Galagan, J. E.; Henn, M. R.; Ma, L. J.; Cuomo, C. A.; Birren, B. Genomics of the fungal kingdom: insights into eukaryotic biology. *Genome Res.* **2005**, *15*, 1620−1631.

(9) Nødvig, C. S.; Nielsen, J. B.; Kogle, M. E.; Mortensen, U. H. A CRISPR-Cas9 System for Genetic Engineering of Filamentous Fungi. *PLoS One* **2015**, *10*, No. e0133085.

(10) Al Abdallah, Q.; Ge, W.; Fortwendel, J. R. A Simple and Universal System for Gene Manipulation in *Aspergillus fumigatus*: *In Vitro*-Assembled Cas9-Guide RNA Ribonucleoproteins Coupled with Microhomology Repair Templates. *mSphere* **2017**, *2*, No. e00446-17.

(11) Pohl, C.; Kiel, J. A. K. W.; Driessen, A. J. M.; Bovenberg, R. A. L.; Nygård, Y. CRISPR/Cas9 Based Genome Editing of *Penicillium chrysogenum*. *ACS Synth. Biol.* **2016**, *5*, 754−764.

(12) Yuan, B.; Keller, N. P.; Oakley, B. R.; Stajich, J. E.; Wang, C. C. C. Manipulation of the Global Regulator mcrA Upregulates Secondary Metabolite Production in *Aspergillus wentii* Using CRISPR-Cas9 with In Vitro Assembled Ribonucleoproteins. *ACS Chem. Biol.* **2022**, *17*, 2828−2835.

(13) Lebar, M. D.; Cary, J. W.; Majumdar, R.; Carter-Wientjes, C. H.; Mack, B. M.; Wei, Q.; Uka, V.; De Saeger, S.; Di Mavungu, J. D.

Identification and functional analysis of the aspergillic acid gene cluster in *Aspergillus flavus*. *Fungal Genet. Biol.* **2018**, *116*, 14−23.
(14) Xu, X.; He, F.; Zhang, X.; Bao, J.; Qi, S. New mycotoxins from marine-derived fungus Aspergillus sp. SCSGAF0093. *Food Chem. Toxicol.* **2013**, *53*, 46−51.
(15) Morales-Sánchez, V.; Díaz, C. E.; Trujillo, E.; Olmeda, S. A.; Valcarcel, F.; Muñoz, R.; Andrés, M. F.; González-Coloma, A. Bioactive Metabolites from the Endophytic Fungus Aspergillus sp. SPH2. *J. Fungi* **2021**, *7*, No. 109.
(16) Zhu, F.; Chen, G.; Chen, X.; Huang, M.; Wan, X. Aspergicin, a new antibacterial alkaloid produced by mixed fermentation of two marine-derived mangrove epiphytic fungi. *Chem. Nat. Compd.* **2011**, *47*, 767−769.
(17) MacDonald, J. C. Toxicity, analysis, and production of aspergillic acid and its analogues. *Can. J. Biochem.* **1973**, *51*, 1311−1315.
(18) Lebar, M. D.; Mack, B. M.; Carter-Wientjes, C. H.; Gilbert, M. K. The aspergillic acid biosynthetic gene cluster predicts neo-aspergillic acid production in Aspergillus section Circumdati. *World Mycotoxin J.* **2019**, *12*, 213−222.
(19) Bao, J.; Wang, J.; Zhang, X. Y.; Nong, X. H.; Qi, S. H. New Furanone Derivatives and Alkaloids from the Co-Culture of Marine-Derived Fungi *Aspergillus sclerotiorum* and *Penicillium citrinum*. *Chem. Biodiversity* **2017**, *14*, No. e1600327.
(20) Guo, C.; Wang, P.; Pang, X.; Lin, X.; Liao, S.; Yang, B.; Zhou, X.; Wang, J.; Liu, Y. Discovery of a Dimeric Zinc Complex and Five Cyclopentenone Derivatives from the Sponge-Associated Fungus *Aspergillus ochraceopetaliformis*. *ACS Omega* **2021**, *6*, 8942−8949.
(21) Zheng, J.; Wang, Y.; Wang, J.; Liu, P.; Li, J.; Zhu, W. Antimicrobial ergosteroids and pyrrole derivatives from halotolerant *Aspergillus flocculosus* PT05-1 cultured in a hypersaline medium. *Extremophiles* **2013**, *17*, 963−971.
(22) Stajich, J.; Palmer, J. Automatic Assembly for the Fungi (AAFTF): Genome Assembly Pipeline, 2022 https://zenodo.org/record/1620526. accessed on September 20, 2022.
(23) Bolger, A. M.; Lohse, M.; Usadel, B. Trimmomatic: a flexible trimmer for Illumina sequence data. *Bioinformatics* **2014**, *30*, 2114−2120.
(24) Prjibelski, A.; Antipov, D.; Meleshko, D.; Lapidus, A.; Korobeynikov, A. Using SPAdes De Novo Assembler. *Curr. Protoc. Bioinf.* **2020**, *70*, No. e102.
(25) Altschul, S. F.; Gish, W.; Miller, W.; Myers, E. W.; Lipman, D. J. Basic local alignment search tool. *J. Mol. Biol.* **1990**, *215*, 403−410.
(26) Brown, C. T.; Irber, L. Sourmash: a library for MinHash sketching of DNA. *J. Open Source Software* **2016**, *1*, No. 27.
(27) Walker, B. J.; Abeel, T.; Shea, T.; Priest, M.; Abouelliel, A.; Sakthikumar, S.; Cuomo, C. A.; Zeng, Q.; Wortman, J.; Young, S. K.; Earl, A. M. Pilon: an integrated tool for comprehensive microbial variant detection and genome assembly improvement. *PLoS One* **2014**, *9*, No. e112963.
(28) Li, H. Minimap2: pairwise alignment for nucleotide sequences. *Bioinformatics* **2018**, *34*, 3094−3100.
(29) Smit, A. F. A.; Hubley, R. RepeatModeler-v1.0. (2008-2015), 2022, http://www.repeatmasker.org. accessed on September 20, 2022.
(30) Love, J.; Palmer, J.; Stajich, J.; Esser, T.; Kastman, E.; Winter, D. Funannotate-v1.5.0, 2018 https://zenodo.org/record/1342272. accessed on September 20, 2022.
(31) Manni, M.; Berkeley, M. R.; Seppey, M.; Zdobnov, E. M. BUSCO: Assessing Genomic Data Quality and Beyond. *Curr. Protoc.* **2021**, *1*, No. e323.
(32) Leskovec, J.; Sosič, R. SNAP: A General Purpose Network Analysis and Graph Mining Library. *ACM Trans. Intell. Syst. Technol.* **2016**, *8*, 1−20.
(33) Stanke, M.; Morgenstern, B. AUGUSTUS: a web server for gene prediction in eukaryotes that allows user-defined constraints. *Nucleic Acids Res.* **2005**, *33*, W465−W467.
(34) Boutet, E.; Lieberherr, D.; Tognolli, M.; Schneider, M.; Bairoch, A. UniProtKB/Swiss-Prot. *Methods in Mol. Biol.* **2007**, *406*, 89−112.
(35) Putz, H.; Brandenburg, K. Diamond-Crystal and Molecular Structure Visualization Crystal Impact *GbR: Bonn, Germany* 2022.
(36) Haas, B. J.; Salzberg, S. L.; Zhu, W.; Pertea, M.; Allen, J. E.; Orvis, J.; White, O.; Buell, C. R.; Wortman, J. R. Automated eukaryotic gene structure annotation using EVidenceModeler and the Program to Assemble Spliced Alignments. *Genome Biol.* **2008**, *9*, No. R7.
(37) Mistry, J.; Chuguransky, S.; Williams, L.; Qureshi, M.; Salazar, G. A.; Sonnhammer, E. L. L.; Tosatto, S. C. E.; Paladin, L.; Raj, S.; Richardson, L. J.; Finn, R. D.; Bateman, A. Pfam: The protein families database in 2021. *Nucleic Acids Res.* **2021**, *49*, D412−D419.
(38) Blum, M.; Chang, H. Y.; Chuguransky, S.; Grego, T.; Kandasaamy, S.; Mitchell, A.; Nuka, G.; Paysan-Lafosse, T.; Qureshi, M.; Raj, S.; et al. The InterPro protein families and domains database: 20 years on. *Nucleic Acids Res.* **2021**, *49*, D344−D354.
(39) Drula, E.; Garron, M. L.; Dogan, S.; Lombard, V.; Henrissat, B.; Terrapon, N. The carbohydrate-active enzyme database: functions and literature. *Nucleic Acids Res.* **2022**, *50*, D571−D577.
(40) Zhang, H.; Yohe, T.; Huang, L.; Entwistle, S.; Wu, P.; Yang, Z.; Busk, P. K.; Xu, Y.; Yin, Y. dbCAN2: a meta server for automated carbohydrate-active enzyme annotation. *Nucleic Acids Res.* **2018**, *46*, W95−W101.
(41) Rawlings, N. D.; Waller, M.; Barrett, A. J.; Bateman, A. MEROPS: the database of proteolytic enzymes, their substrates, and inhibitors. *Nucleic Acids Res.* **2014**, *42*, D503−D509.
(42) Huerta-Cepas, J.; Szklarczyk, D.; Heller, D.; Hernández-Plaza, A.; Forslund, S. K.; Cook, H.; Mende, D. R.; Letunic, I.; Rattei, T.; Jensen, L. J.; et al. eggNOG 5.0: a hierarchical, functionally and phylogenetically annotated orthology resource based on 5090 organisms and 2502 viruses. *Nucleic Acids Res.* **2019**, *47*, D309−D314.
(43) Blin, K.; Wolf, T.; Chevrette, M. G.; Lu, X.; Schwalen, C. J.; Kautsar, S. A.; Duran, H. G. S.; de Los Santos, E.; Kim, H. U.; Nave, M.; et al. antiSMASH 4.0-improvements in chemistry prediction and gene cluster boundary identification. *Nucleic Acids Res.* **2017**, *45*, W36−W41.
(44) Houbraken, J.; Visagie, C. M.; Frisvad, J. C. Recommendations To Prevent Taxonomic Misidentification of Genome-Sequenced Fungal Strains. *Microbiol. Resour. Announce.* **2021**, *10*, No. e0107420.
(45) Edgar, R. C. Muscle5: High-accuracy alignment ensembles enable unbiased assessments of sequence homology and phylogeny. *Nat. Commun.* **2022**, *13*, No. 6968.
(46) Capella-Gutiérrez, S.; Silla-Martínez, J. M.; Gabaldón, T. trimAl: a tool for automated alignment trimming in large-scale phylogenetic analyses. *Bioinformatics* **2009**, *25*, 1972−1973.
(47) Minh, B. Q.; Schmidt, H. A.; Chernomor, O.; Schrempf, D.; Woodhams, M. D.; von Haeseler, A.; Lanfear, R. IQ-TREE 2: New Models and Efficient Methods for Phylogenetic Inference in the Genomic Era. *Mol. Biol. Evol.* **2020**, *37*, 1530−1534.
(48) Manni, M.; Berkeley, M. R.; Seppey, M.; Simão, F. A.; Zdobnov, E. M. BUSCO Update: Novel and Streamlined Workflows along with Broader and Deeper Phylogenetic Coverage for Scoring of Eukaryotic, Prokaryotic, and Viral Genomes. *Mol. Biol. Evol.* **2021**, *38*, 4647−4654.
(49) Eddy, S. R. Accelerated Profile HMM Searches. *PLoS Comput. Biol.* **2011**, *7*, No. e1002195.
(50) Price, M. N.; Dehal, P. S.; Arkin, A. P. FastTree 2–approximately maximum-likelihood trees for large alignments. *PLoS One* **2010**, *5*, No. e9490.
(51) The PHYling pipeline, 2022 https://github.com/stajichlab/PHYling_unified. accessed on September 20, 2022.
(52) Steenwyk, J. L.; Buida, T. J.; Labella, A. L.; Li, Y.; Shen, X. X.; Rokas, A. PhyKIT: a broadly applicable UNIX shell toolkit for processing and analyzing phylogenomic data. *Bioinformatics* **2021**, *37*, 2325−2331.
(53) Steenwyk, J. L.; Buida, T. J.; Gonçalves, C.; Goltz, D. C.; Morales, G.; Mead, M. E.; LaBella, A. L.; Chavez, C. M.; Schmitz, J.

https://doi.org/10.1021/acsomega.2c08104
ACS Omega 2023, 8, 16713−16721

E.; Hadjifrangiskou, M.; Li, Y.; Rokas, A. BioKIT: a versatile toolkit for processing and analyzing diverse types of sequence data. *Genetics* **2022**, *221*, No. iyac079.

https://doi.org/10.1021/acsomega.2c08104
ACS Omega 2023, 8, 16713−16721